

The proteolysis adaptor, NblA, initiates protein pigment degradation by interacting with the cyanobacterial light-harvesting complexes

Eleonora Sendersky¹, Noga Kozler¹, Mali Levi¹, Yuval Garini², Yaron Shav-Tal¹ and Rakefet Schwarz^{1,*}

¹The Mina and Everard Goodman Faculty of Life Sciences, Bar-Ilan University, Ramat-Gan 5290002, Israel, and

²Physics Department, Bar-Ilan University, Ramat-Gan 5290002, Israel

Received 13 January 2014; revised 3 April 2014; accepted 25 April 2014; published online 2 May 2014.

*For correspondence (e-mail Rakefet.Schwarz@biu.ac.il)

SUMMARY

Degradation of the cyanobacterial protein pigment complexes, the phycobilisomes, is a central acclimation response that controls light energy capture. The small protein, NblA, is essential for proteolysis of these large complexes, which may reach a molecular mass of up to 4 MDa. Interactions of NblA *in vitro* supported the suggestion that NblA is a proteolysis adaptor that labels the pigment proteins for degradation. The mode of operation of NblA *in situ*, however, remained unresolved. Particularly, it was unclear whether NblA interacts with phycobilisome proteins while part of the large complex, or alternatively interaction with NblA, necessitates dissociation of pigment subunits from the assembly. Fluorescence intensity profiles demonstrated the preferential presence of NblA::GFP (green fluorescent protein) at the photosynthetic membranes, indicating co-localization with phycobilisomes. Furthermore, fluorescence lifetime imaging microscopy provided *in situ* evidence for interaction of NblA with phycobilisome protein pigments. Additionally, we demonstrated the role of NblA *in vivo* as a proteolysis tag based on the rapid degradation of the fusion protein NblA::GFP compared with free GFP. Taken together, these observations demonstrated *in vivo* the role of NblA as a proteolysis adaptor. Additionally, the interaction of NblA with phycobilisomes indicates that the dissociation of protein pigment subunits from the large complex is not a prerequisite for interaction with this adaptor and, furthermore, implicates NblA in the disassembly of the protein pigment complex. Thus, we suggest that, in the case of proteolysis of the phycobilisome, the adaptor serves a dual function: undermining the complex stability and designating the dissociated pigments for degradation.

Keywords: Regulated proteolysis, phycobilisome, adaptor protein, cyanobacteria, *Synechococcus elongatus* PCC 7942.

INTRODUCTION

Light absorbance by photosynthetic organisms is continuously adjusted to ambient conditions to provide efficient light harvesting and avoid the photoinhibitory effect of excess excitation (Vass and Aro, 2007; Bailey and Grossman, 2008; Kehoe, 2010; Nixon *et al.*, 2010; Nowaczyk *et al.*, 2010; Kirilovsky and Kerfeld, 2012; Muramatsu and Hihara, 2012; Tikkanen *et al.*, 2012). Phycobilisomes are large protein pigment complexes that serve the purpose of light harvesting in cyanobacteria and red algae (Glazer, 1985; Gantt, 1994; Ting *et al.*, 2002; Tandeau, 2003; Adir, 2005; Six *et al.*, 2007; Mullineaux, 2008; Su *et al.*, 2010; Watanabe and Ikeuchi, 2013). Degradation of these complexes is a pivotal acclimation response to nutrient limitation (Allen and Smith, 1969; Grossman *et al.*, 1993, 2001; Schwarz and Forchhammer, 2005). A small protein, NblA,

which is essential for the regulated proteolysis of the phycobilisome, was initially identified in the cyanobacterium *Synechococcus elongatus* PCC 7942 (Collier and Grossman, 1994). The designation, NblA, reflects the 'non-bleaching' phenotype of the knockout-mutant, which remains blue-green under conditions that trigger phycobilisome degradation, in contrast with the wild type that turns yellowish or bleaches. Orthologs of NblA of *S. elongatus* (proteins of ~6–7 kDa) have been identified in a variety of cyanobacteria and red algae (Baier *et al.*, 2001, 2004; Richard *et al.*, 2001; Li and Sherman, 2002; Luque *et al.*, 2003; de Alda *et al.*, 2004; Kawakami *et al.*, 2009). Transcription of *nblA*, which is induced by specific environmental cues, is subject to complex and tight regulation (Schwarz and Grossman, 1998; Sauer *et al.*, 1999; Luque

et al., 2001; van Waasbergen *et al.*, 2002; Osanai *et al.*, 2005; Sendersky *et al.*, 2005; Lahmi *et al.*, 2006; Salinas *et al.*, 2007; Zabulon *et al.*, 2007; Kato *et al.*, 2008, 2011; Ruiz *et al.*, 2008; Leganes *et al.*, 2009). Recently, homologs of NblA were identified in the genomes of cyanophages (Yoshida *et al.*, 2008; Gao *et al.*, 2012; Yoshida-Takashima *et al.*, 2012; Nakamura *et al.*, 2014), however, the role of these viral *nblA* genes in phage infection is yet unknown.

Phycobilisomes are large water-soluble protein pigment assemblies, which are anchored to the photosynthetic membranes. A recent study demonstrated the presence of a megacomplex resulting from the interaction of the phycobilisome with the membrane located photosynthetic reaction center complexes (Liu *et al.*, 2013). The phycobilisome is comprised of pigment binding-proteins (phycobiliproteins) as well as linker proteins, most of which do not bind chromophores. Phycobiliprotein dimers, which are considered to be the basic, so-called monomeric building block of the pigment complex, assemble into trimeric rings, which are further stacked to yield cylindrical shapes. Short cylinders of the pigment protein allophycocyanin, comprise the core of the complex, whereas cylindrical assemblies of other pigments, (e.g. phycocyanin) emanate from the core, giving rise to a hemi-discoidal structure. The particular pigment composition varies between species and in response to light conditions (Glazer, 1985; Gantt, 1994; Grossman *et al.*, 1995; MacColl, 1998; Adir, 2005; Watanabe and Ikeuchi, 2013).

Substrate recognition in bacterial proteolysis relies, in particular cases, on adaptor proteins that interact with the substrate and introduce it to the degradation machinery (Mogk *et al.*, 2007; Ades, 2008; Hengge, 2009; Kirstein *et al.*, 2009; Schmidt *et al.*, 2009; Tyedmers *et al.*, 2010; Gur *et al.*, 2011; Sauer and Baker, 2011; Dougan *et al.*, 2012; Battesti and Gottesman, 2013). Such a tagging function, which was initially postulated for NblA (Collier and Grossman, 1994), was corroborated by affinity purification experiments demonstrating interaction, *in vitro*, of NblA from the cyanobacteria *Tolypothrix* PCC 7601 and *Anabaena* PCC 7120 with phycobilisome protein pigments (Luque *et al.*, 2003; Bienert *et al.*, 2006). Additionally, NblA of *Anabaena* was shown to interact *in vitro* with ClpC, a chaperone subunit of the clp protease complex (Karradt *et al.*, 2008). The protein degradation machinery of chloroplasts employs clp proteases, in accordance with the cyanobacterial origin of these organelles (Adam *et al.*, 2006; Olinares *et al.*, 2011; Clarke, 2012).

Interaction of NblA, *in vitro*, with phycobilisome protein pigments and with ClpC, provided support for the suggested function of NblA as an adaptor of proteolysis. The mode of action of NblA *in vivo*, however, remained unresolved. In principle, two basic scenarios may be envisaged for designation of protein pigments of the phycobilisome for degradation. In the first one, NblA initially interacts

with the protein pigments while they are part of the large light-harvesting pigment complex. Alternatively, it may be suggested that while part of the phycobilisome assembly, the protein pigments are inaccessible to NblA. Therefore, detachment of small pigment subunits (e.g. monomers or trimers) from the phycobilisome is required prior to interaction with NblA. Here, using an NblA::GFP fusion protein, we present evidence for interaction of NblA with intact phycobilisomes, thereby assigning to NblA a role in the supra-complex disassembly. Furthermore, the role of NblA as a degradation tag is demonstrated *in vivo*, based on the rapid degradation of the fusion protein NblA::GFP.

RESULTS AND DISCUSSION

Cellular localization of NblA::GFP

To determine the initial target of interaction of NblA, we followed its localization *in situ*. To this end, a gene encoding GFP-labeled NblA was introduced into NblA Ω , the *nblA*-inactivated strain of *S. elongatus* (NblA::GFP, Figure 1(a)). This fusion product restored phycobilisome degradation in NblA Ω , under nitrogen starvation conditions, as indicated by the level of phycocyanin, the major pigment of the light-harvesting antenna of *S. elongatus* (Figure 1b). The strain expressing the NblA::GFP exhibited slower phycocyanin degradation relative to a strain possessing native NblA (Figure 1(b), compare NblA::GFP and the Free GFP strain following 48 h of nitrogen starvation). Phycocyanin levels, however, were comparable in these strains when starvation was prolonged to 96 h (Figure 1b), indicating that tagging of NblA with GFP does not abrogate its function.

Fluorescence microscopy was used to determine the cellular localization of NblA::GFP. In *S. elongatus* as in some other cyanobacteria, the photosynthetic membranes are arranged in multiple shells that lie underneath the cell membrane leaving a central membrane-free area [(Mullineaux, 1999; Liberton *et al.*, 2006; van de Meene *et al.*, 2006; Nevo *et al.*, 2007), also see Figure 2(c)]. Perforations in these membranes allow trafficking of water-soluble molecules throughout the cell (Nevo *et al.*, 2007). Upon excitation of the phycobilisome, an ellipse-shaped red fluorescent region was revealed, reflecting the arrangement of the photosynthetic membranes, which was manifested in the intensity profile across the cell, as two regions of intense red fluorescence enclosing a relatively dim region (Figure 2(a,b), red traces). Notably, cells expressing NblA::GFP exhibited a similar profile of green fluorescence (Figure 2a), in contrast with the free GFP strain, which was characterized by bright green fluorescence, evenly dispersed throughout the cell (Figure 2b). Emission spectra confirmed the presence of GFP in the NblA::GFP and the Free GFP strains. The spectra of these strains were characterized by emission maximum at 505 nm, close to the

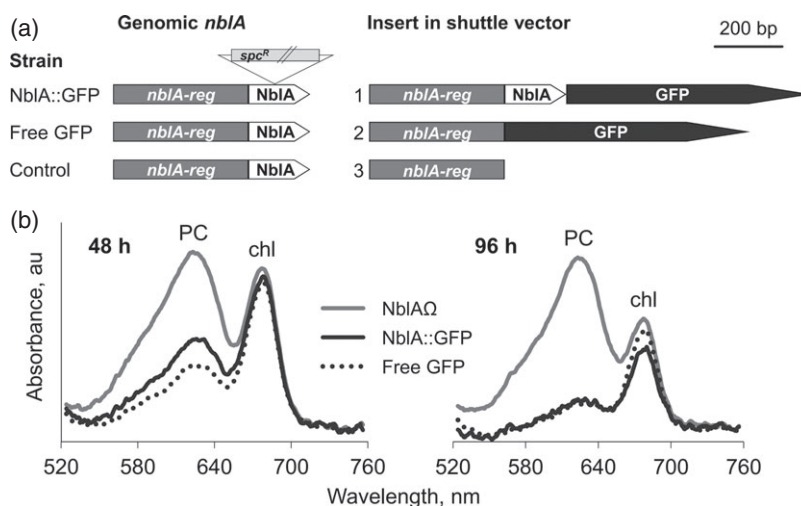


Figure 1. NblA::GFP restores phycocyanin degradation to the *nblA*-inactivated strain.

(a) Constructs used to study the cellular role of NblA. NblA::GFP: The coding region of GFP was fused to the C-terminus of NblA. The regulatory region of *nblA* (*nblA-reg*) includes 400 bp upstream of the start codon of NblA. This fragment includes the promoter of *nblA* and its putative ribosome binding site. Free GFP: The open reading frame (ORF) encoding GFP was attached to the regulatory region of *nblA*. NblA::GFP and free GFP were introduced into the *nblA*-mutant (NblA Δ) and wild type cells, respectively. Thus, each of the resulting strains harbors a single intact *nblA* gene. As a control strain, we used wild type cells that contained *nblA-reg* in a shuttle vector (referred to throughout the study as wild type). *spc^R* –spectinomycin resistance cassette.

(b) Changes in cell pigmentation following 48 h or 96 h of nitrogen starvation detected by absorbance spectra of cell cultures. Strains included in the analyses: *nblA*-inactivated (NblA Δ); NblA::GFP, and free GFP. Absorbance maximum at 620 nm indicated phycocyanin (PC), the major component of the light-harvesting complex in *Synechococcus elongatus*. Absorbance maximum at 680 nm reflected the chlorophyll (chl) level. Phycocyanin degradation progressed more slowly in NblA::GFP compared with the free GFP strain; following 96 h starvation, however, phycocyanin levels were similar in these two strains. Absorbance is shown in arbitrary units (au).

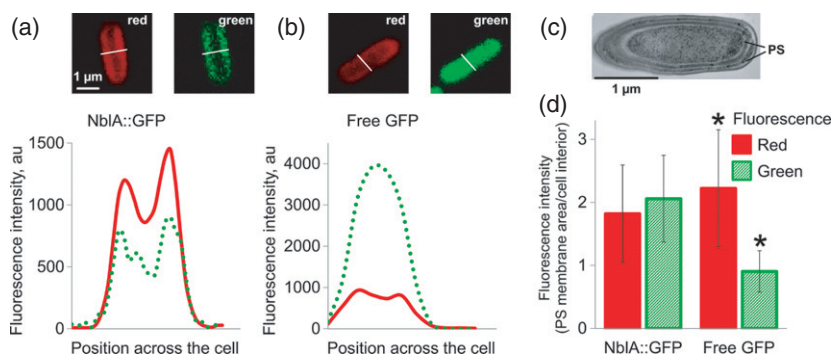


Figure 2. NblA::GFP is preferentially localized to the photosynthetic membranes.

(a, b) Confocal fluorescence images and fluorescence intensity profiles of NblA::GFP and the free GFP strains. The white line across each cell image indicates the region at which the intensity profile was measured. Cells were excited at 488 nm, and emission was recorded at: 620–670 nm (red solid lines); 500–530 nm (green dotted lines). Note the different intensity scale for the strain that expressed free GFP. Fluorescence intensity is shown in arbitrary units (au).

(c) Electron micrographs of longitudinal section of an *Synechococcus elongatus* cell that demonstrated the organization of the photosynthetic membranes (PS). The image was obtained from high pressure-frozen, freeze-substituted cell samples.

(d) Quantitative analysis of cell fluorescence: signal from the membrane area was divided by that from the cell interior (average and standard deviation of 25 and 28 cells, for NblA::GFP and free GFP, respectively). The asterisk indicates statistical significance (*t*-test $P < 0.05$).

commonly reported emission maximum of GFP (508–510 nm), whereas wild-type cells exhibited a very low signal in this emission range (Figure S1).

The fluorescence intensity measurements were then used to derive the ratio between the signal intensity in the region of the photosynthetic membranes and the cell interior (see details in Experimental Procedures). Average ratio of ~1 indicates an even distribution between the

membrane region and the cell interior. The average ratio of the red fluorescence, however, was ~2 (Figure 2d) for free GFP as well as the NblA::GFP strains, consistent with the phycobilisomes being located at the photosynthetic membranes at the cell periphery. In the free GFP strain, the average ratio of green fluorescence was ~1 (Figure 2d), indicating that free GFP was dispersed evenly throughout the cell. In contrast, the NblA::GFP strain was characterized

by an average ratio of green fluorescence of ~ 2 (Figure 2d), indicating preferential presence of the fusion protein at the photosynthetic membranes. These data support a model in which the process of pigment degradation is initiated by interaction of NblA with phycobilisomes. An alternative mode of operation assumes detachment of small phycocyanin assemblies (e.g. monomers or trimers) prior to the interaction with NblA. Dissociated pigments will diffuse and disperse throughout the cell as demonstrated here for *S. elongatus* (Figure S4, see details in Experimental Procedures) as well as was previously shown for *Synechocystis* PCC 6803 (Tamary *et al.*, 2012). This putative scenario of phycobilisome dissociation is expected to result in an evenly distributed GFP fluorescence in the NblA::GFP strain, contrary to our observations (Figure 2a,d).

NblA::GFP is characterized by a shorter fluorescence lifetime compared with free GFP

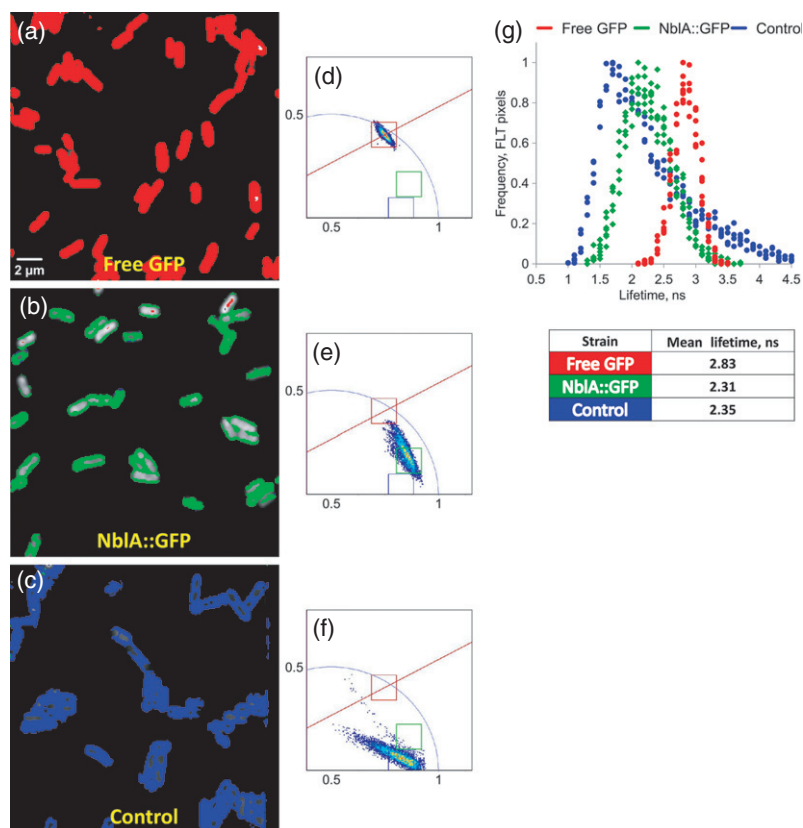
Förster Resonance Energy Transfer (FRET) implemented through fluorescence lifetime imaging microscopy (FLIM) was employed to assess further the molecular interactions of NblA *in situ*. This technique enables detection of protein–protein interactions, in which shortening of the fluorescence lifetime of the donor indicates energy transfer to the acceptor (see Experimental Procedures). The fluorescence lifetime is measured at every pixel of the image and

therefore allocates regions of co-localization of the donor and the acceptor. We hypothesized that an interaction of GFP-labeled NblA with the phycobilisome may bring GFP to the vicinity of a pigment (phycocyanin or allophycocyanin). Sufficiently close apposition that would allow for energy transfer from GFP to the pigment would be reflected in a shorter fluorescence lifetime of GFP. The emission spectrum of GFP, the putative donor, and absorbance spectra of phycocyanin and allophycocyanin, the putative acceptors, indicated spectral overlap (Figure S2). This spectral overlap, although not ideal, is compensated for by the vast abundance of phycobilisome pigments and their organization into multimeric complexes. Such organization of the pigments into supramolecular complexes may allow NblA to be surrounded by several pigment molecules, thereby increasing the probability of energy transfer. To detect possible energy transfer between GFP and the phycobilisome pigments, we compared the fluorescence lifetime of free GFP and NblA::GFP expressed in *S. elongatus*. Fluorescence lifetime images are presented using the phasor approach where each pixel of the image gives a point in the phasor plot. Image analysis is based on clustering of pixels in specific regions of the plot (see Experimental Procedures and legend to Figure 3).

Free GFP expressed in *S. elongatus* cells exhibited a mean fluorescence lifetime of 2.83 ns (Figure 3g), within

Figure 3. Fluorescence lifetime images (a–c) and phasor plots (d–f) of the following strains: Free GFP (a, d); NblA::GFP (b, e) and the control strain (c, f).

The phasor analyses represent lifetime data as density plots (red, yellow, light blue and dark blue represent decreasing densities). Colored squares define subsets of lifetime pixels. These, so-called regions of interest were selected to define the majority of the data of free GFP (red), NblA::GFP (green) and the control strain (blue). Once placed on the phasor plot, these regions of interest served for analysis of all images. Scale bar in (a) (2 μm) is relevant to images shown in (a–c). In 38% of the control cells ($n = 68$) the autofluorescence was confined to the region of the photosynthetic membranes. (g) Histograms of the time delays of data shown in (a–c). Data were normalized at the maximal frequency. Mean fluorescence lifetimes were calculated from data obtained from three different microscope fields for each strain. Analysis of variance (ANOVA) with the Bonferroni *post hoc* test indicated significant difference between populations of the three strains $P < 0.0001$ ($F = 9416.5$, $df = 2, 97784$).



the range of values reported for GFP (Scruggs *et al.*, 2005). In contrast with the free GFP strain, the NblA::GFP strain was characterized by a wider range of fluorescence lifetimes (compare Figure 3(d,e), respectively as well as red and green histograms in Figure 3(g)). Importantly, the mean fluorescence lifetime calculated for NblA::GFP, 2.31 ns (Figure 3g), was significantly shorter compared with the lifetime obtained for free GFP, indicating substantial FRET in the NblA::GFP strain. This energy transfer indicated that NblA::GFP was localized in close vicinity to the phycobilisome pigments. Furthermore, 87% of the NblA::GFP-expressing cells ($n = 149$) demonstrated a fluorescence lifetime pattern reminiscent of the photosynthetic membranes enclosing the cell interior (see for example Figure 3(b)). In contrast with the NblA::GFP strain, in 90% of the cells that expressed free GFP ($n = 96$) the lifetime pixels were distributed evenly throughout the cells (Figure 3a). The localization of the short fluorescence lifetime pixels in the NblA::GFP strain to the region of the photosynthetic membranes supported the association of NblA with the phycobilisome.

The autofluorescence detected in the control cells was characterized by a mean lifetime of 2.35 ns (Figure 3c,f,g). Our data indicated distinct characteristics of fluorescence lifetimes of the control strain and the GFP-expressing strains. First, the lifetime distributions were markedly different between the NblA::GFP strain and the background measured for the control strain. For NblA::GFP, the lifetimes were distributed symmetrically in contrast with the broad and asymmetric distribution of the control data (Figure 3(g) green and blue histograms, respectively), confirming that the measured lifetimes corresponded to the NblA::GFP fluorescence lifetime. Second, as apparent from the phasor plot, lifetime data of the control strain deviated from the line that connected the lifetime pixels of the GFP-

expressing strains (Figure 3f), a result that indicated that the lifetimes are related to different populations (Clayton *et al.*, 2004; Digman *et al.*, 2008). Altogether, these data demonstrated that GFP lifetimes are clearly distinguished from the background, and supported the conclusion that the shorter lifetime measured for NblA::GFP compared with free GFP represented FRET.

Free GFP or NblA::GFP was also expressed in *Escherichia coli* cells to examine the fluorescence lifetimes of these proteins in a cell that does not harbor the putative acceptors for energy transfer. The mean fluorescence lifetime of NblA::GFP measured in *E. coli* was 4.05 ns, significantly longer than the 3.15 ns obtained for free GFP expressed in these cells (Figure S3). These data indicated that shortening of the fluorescence lifetime of NblA::GFP compared with free GFP that is measured in the cyanobacterial cells, reflected energy transfer between GFP and protein pigments of the phycobilisome and not merely an intrinsic property of the fusion protein. The mean fluorescence lifetime of free GFP in *E. coli*, 3.15 ns compared with 2.83 ns in *S. elongatus* (Figures S3 and 3(g), respectively), may reflect the effect of the different cellular environment.

NblA::GFP is degraded rapidly compared with free GFP

Fluorescence microscopy indicated relatively low green fluorescence signal in NblA::GFP cells compared with cells of the free GFP strain (Figure 2(a,b), note different y axis). Fluorescence measurements of bulk cultures of these strains corroborated this difference in green fluorescence intensity (Figure 4a). Furthermore, the level of free GFP, as revealed by western blot analysis, was substantially higher compared with the fusion product NblA::GFP (Figure 4(b), compare signals at 48 h starvation). In light of these observations, we postulated that NblA may designate the attached GFP to proteolysis, and the lower steady-state

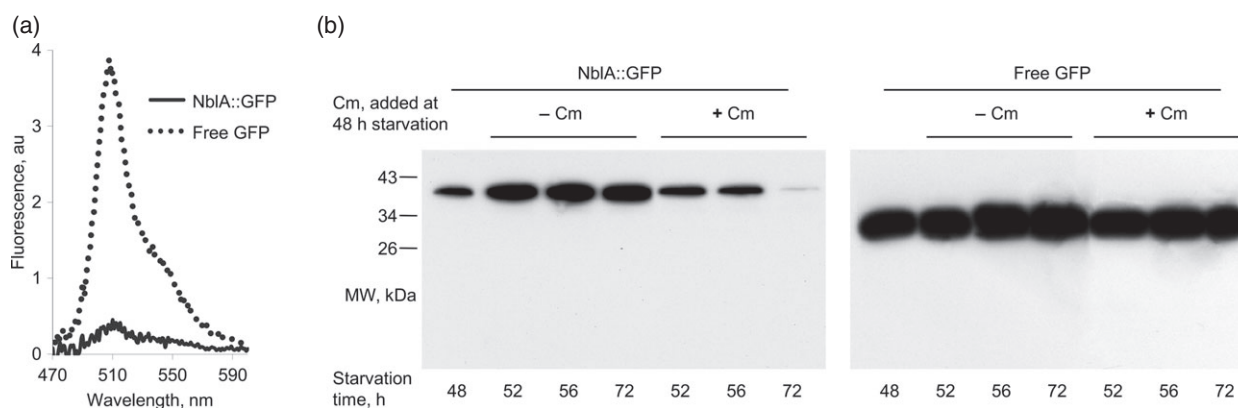


Figure 4. NblA::GFP exhibits rapid degradation compared with free GFP.

(a) Fluorescence spectra of cultures of the NblA::GFP and the free GFP strains.

(b) Western blot analysis using anti-GFP. Cells were starved for nitrogen for 48 h to induce expression from the *nblA* promoter and to enable accumulation of free GFP and NblA::GFP. Then, chloramphenicol (Cm) was added to inhibit protein synthesis and the level of the free reporter and the fusion product NblA::GFP in cell extracts was determined at the indicated times.

level of the fusion protein, results at least in part, from its rapid degradation. To examine the stability of free GFP versus that of NblA::GFP, we inhibited protein synthesis using chloramphenicol (Cm), and followed the levels of these proteins by western blot analysis. NblA::GFP exhibited rapid degradation in contrast with free GFP, which under the same experimental conditions, was not degraded over the time course tested (Figure 4b). These data suggest that the fusion protein NblA::GFP is introduced to the cellular degradation machinery. The degradation of NblA::GFP may suggest that NblA, by itself, is degraded. Support for this hypothesis is provided by *in vitro* experiments that demonstrated proteolysis of NblA of *Synechocystis* PCC 6803 by a clp protease complex (Baier *et al.*, 2014).

In summary, this study included different experimental approaches that demonstrated, *in vivo*, the function of NblA as an adaptor of proteolysis. The short fluorescence lifetime that characterized the NblA::GFP strain compared with free GFP (Figure 3) supported the interaction of NblA with phycobilisome pigments. Furthermore, fluorescence intensity profiles (Figure 2) and the cell images obtained from the FRET-FLIM analyses (Figure 3b) indicated preferential localization of NblA::GFP to the photosynthetic membranes and supported interaction of NblA with phycobilisomes. Additionally, the rapid degradation of NblA::GFP compared with free GFP (Figure 4) denoted that NblA was capable of designating the fusion protein to proteolysis.

Degradation of a large complex such as the phycobilisome may require dissociation of monomers or small sub-complex assemblies to allow interaction with the adaptor protein. In an alternative scenario, NblA may be able to associate with the large complex and thereby initiate the degradation process. Intensity profiles (Figure 2), as well as the patterning of the fluorescence lifetime data (Figure 3) that demonstrated the presence of NblA::GFP at the photosynthetic membranes and co-localization with phycobilisomes, supported a model in which NblA is intertwined into the large protein pigment complex. This model implied that the proteolysis adaptor is also involved in the pigment complex disassembly. Several functions were postulated for NblA upon its identification including a role in phycobilisome disassembly (Collier and Grossman, 1994) and, later on, based on its crystal structure, NblA was predicted to intercalate into the phycobilisome structure and to undermine the association of neighboring phycocyanin subunits (Dines *et al.*, 2008). The current study provides solid evidence for such a disassemblase function; interaction of NblA with phycobilisomes associated with the photosynthetic membranes, and supports a scenario in which the small adaptor protein assists in dissociation of the pigment complex. We propose that small assemblies of phycobilisome pigments and NblA are detached from the whole pigment complex and that the pigments are further designated to degradation.

EXPERIMENTAL PROCEDURES

Strains, culture conditions

Synechococcus elongatus PCC 7942 and derived strains were grown as described previously (Schatz *et al.*, 2012). Strains that carried a shuttle vector were grown in liquid culture supplemented with $10 \mu\text{g ml}^{-1}$ kanamycin or spectinomycin, as appropriate ($5 \mu\text{g ml}^{-1}$ under starvation). Starvation was performed by replacing the replete growth medium with nitrate-lacking medium as follows: cells grown in complete growth medium to an OD_{750} of 0.8–1, were harvested by centrifugation (5000 *g*, 10 min), resuspended in an equal volume of medium that lacked nitrate, re-pelleted by centrifugation, and resuspended in medium that lacked nitrogen to 1/10 of the original culture volume. This concentrated cell culture was diluted into medium that lacked nitrate to an OD_{750} of 0.5. Unless indicated differently, cells were starved for 48 h. At this time point, phycobilisomes were not yet completely degraded (Figure 1b), while sufficient level of NblA::GFP was accumulated to allow microscope analyses.

Escherichia coli DH5 α transformed with pASK-IBA3 (IBA) was used as a control strain. Details of cloning of GFPuv (referred to as GFP) and NblA::GFP in pASK-IBA3 under the *tet* promoter are provided in Table S1. Induction was performed following growth of *E. coli* cultures to an OD_{660} of 0.1 and the addition of $0.2 \mu\text{g ml}^{-1}$ anhydrotetracycline. Molecular details of construction of the strains used in this study are provided in Table S1.

Western blot analysis

Preparation of cell extracts and western blot analysis were performed as described previously (Balint *et al.*, 2006). Chloramphenicol was added following 48 h of nitrogen starvation to a final concentration of $250 \mu\text{g ml}^{-1}$. Mouse monoclonal antibody GFP (Covance, <https://store.crpinc.com/datasheet.aspx?Catalogno=MMS-118R>) and anti-mouse IgG, conjugated to horse radish peroxidase (Jackson ImmunoResearch, http://www.jacksonimmuno.com/MERCHANT2/merchant.mv?Screen=BASK&Store_Code=JI&Action=ADPR&Product_Code=115-035-062&Attributes=Yes&Quantity=1) were used for detection of GFP.

Absorbance and fluorescence measurements and cell imaging

Absorbance was measured using a Carry100 Spectrophotometer (Agilent Technologies, <http://www.chem.agilent.com/en-US/products-services/Instruments-Systems/Molecular-Spectroscopy/Cary-100-UV-Vis/Pages/default.aspx>) equipped with an integrating sphere. Fluorescence from cell cultures was recorded using AB2 Luminescence Spectrometer, Version 5.50 (excitation was provided at 405 nm). For bulk fluorescence measurements, cultures were adjusted to an OD_{750} of 0.8. Olympus FV1000 confocal microscope was used to record fluorescence intensity from individual cells. In preliminary experiments that were performed on non-fixed cells, we observed dispersion of phycobilisome fluorescence during data recruitment. This dispersion was manifested as a loss of the preferential localization of phycobilisome fluorescence to the photosynthetic membranes and increased fluorescence in the internal region of the cell (Figure S4, see legend for details). A similar phenomenon has been reported for the cyanobacterium *Synechocystis* PCC 6803 (Tamary *et al.*, 2012). Further microscope analyses were performed on fixed cells to prevent alterations occurring during image recruitment. Upon sampling, cells were treated with 1% formaldehyde for 2 h at room temperature, and rinsed three times with double-distilled water. Microscope

analyses were performed using glass-bottomed dishes (MatTek, P35GCOL-1.5-14-C, http://glass-bottom-dishes.com/catalog/index.php?main_page=product_info&products_id=48). A drop of 3 μ l of the culture was spotted on the bottom coverslip and spreaded with a slice of 1.5% solidified agar.

Fluorescence excitation was provided at 635 nm to detect phycobilisome preferentially, and the emitted fluorescence was measured at 645–655 nm (red channel). GFP was excited at 488 nm, although we employed GFPuv, as cell excitation at 405 nm (close to the excitation maximum of GFPuv) caused severe bleaching. Emission was detected at the range of 500–525 nm (green channel). As described in the Results, cells of the GFP strain were characterized by high green fluorescence. Therefore, to avoid signal saturation, the intensity of the 488 laser was reduced 10-fold for measurements of the free GFP strain compared with the control and the NblA::GFP strains. Images were acquired at 512 \times 512 pixels. The image processing package, Fiji, was used for image analysis. Fluorescence intensity in the red as well as in the green channel varied between individual cells, therefore to provide a quantitative measure for the fluorescence pattern we calculated the ratio between the maximal and the minimal red fluorescence values. The ratio of green fluorescence was calculated by dividing the relevant values at the same cell positions that yielded the red maximal and minimal fluorescence. The obtained fluorescence ratios, [denoted 'fluorescence intensity, photosynthetic (PS) membrane area/cell interior'], were calculated for 25 and 28 cells, for NblA::GFP and free GFP, respectively (Figure 2d).

FRET-FLIM was employed to examine the interaction between NblA and phycobilisome pigments. This approach maps the spatial distribution of probe lifetimes in individual cells and allows deducing protein–protein interactions based on shortening of the lifetime of the donor molecule (Sun *et al.*, 2011; Bakker *et al.*, 2012). Our working hypothesis assumed that close apposition of NblA and phycocyanin or allophycocyanin should place GFP of the NblA::GFP fusion in close proximity to the pigment and would result in energy transfer between GFP and the protein pigment. Intensity-based FRET was not feasible due to the high abundance of phycocyanin and strong cross-excitation; very high phycocyanin fluorescence was obtained from GFP-lacking strains upon 'specific' GFP excitation at 488 nm. The FRET-FLIM approach offers a methodology that does not involve the drawback of cross-excitation relevant to intensity-based measurements (Sun *et al.*, 2011; Bakker *et al.*, 2012).

FRET-FLIM data were obtained using PicoQuant Microtime 200 system (<http://www.picoquant.com/products/category/fluorescence-microscopes/microtime-200-time-resolved-confocal-fluorescence-microscope-with-unique-single-molecule-sensitivity>) with short-pulsed excitation at 470 nm and emission at 520/35 nm. Excitation intensity in the case of the free GFP strain was tuned to obtain emission intensity similar to the NblA::GFP strain. The PicoQuant Microtime 200 is coupled to a FV1000 confocal microscope and therefore allows measuring the lifetime at every voxel that is scanned. Measurements were performed with a \times 60 magnification (NA = 1.35) objective lens that provided a spatial resolution of 180 nm. For statistical analysis, data from three fields for each of the strains analyzed were used to obtain histograms of the time delays and analysis of variance (ANOVA) with the Bonferroni *post hoc* test was performed.

Time-correlated single photon counting (TCSPC) was used to measure the fluorescence lifetime. In TCSPC an avalanche photodiode (APD) records times at which individual photons are detected after a single excitation pulse from individual pixels. The recordings were repeated for multiple pulses and a decay curve of the number of events across time was generated. The decay curve

may be fitted to a mathematical model to extract time constant(s) – the lifetime values. The challenge in fitting TCSPC FLIM data stems from the following: (i) a relatively small number of photons is collected from a single pixel of an image; and (ii) the decay curves are often complex and contain more than a single population. To avoid the difficulties associated with fitting of the fluorescence decay data using exponentials, FLIM data were processed by the phasor approach using the simFCS software developed by Gratton (Digman *et al.*, 2008; Sun *et al.*, 2011) at the Laboratory for Fluorescence Dynamics (<http://www.lfd.uci.edu/>). This method was first developed for analysis of frequency domain FLIM (Clayton *et al.*, 2004) and adopted later for time domain FLIM by Digman and colleagues (Digman *et al.*, 2008; Sun *et al.*, 2011). The phasor approach transforms the decay curves at each pixel to sine and cosine values according to the following expressions:

$$g_{ij}(\omega) = \int_0^{\infty} I_{ij}(t) \cos(\omega t) dt / \int_0^{\infty} I_{ij}(t) dt$$

$$s_{ij}(\omega) = \int_0^{\infty} I_{ij}(t) \sin(\omega t) dt / \int_0^{\infty} I_{ij}(t) dt$$

where ω is the laser repetition angular frequency and the indexes *i* and *j* identify a pixel of the image. The *s* and *g* coordinates are plotted to generate the phasor plot where lifetime values in each pixel are now presented as a point in a 2D graph. Every molecular species has a specific position on the phasor plot, thus molecules are identified by their particular location and FRET information is obtained by localizing the position of clusters of pixels on the plot (for example see 'regions of interest' in Figure 3). For a FRET pair (NblA::GFP and phycobilisome protein pigments in this case), in which the presence of the acceptor reduces the lifetime of the donor, the resulting phasor of the interacting species (NblA::GFP) cannot lie along the line connecting the phasor of the free GFP and that of the cyanobacterial autofluorescence. The quenched species will be positioned in a different part of the phasor plot (Digman *et al.*, 2008).

For analysis of single cell fluorescence lifetime images, Fiji was used to draw a line across the cell (similar to the line shown in intensity profiles, Figure 2(a,b), and lifetime values across the cells were obtained. Individual cell profiles were normalized to the lowest lifetime value in the particular cell. A flat profile (values <1.25) was considered 'evenly distributed lifetime data'. Fluctuations resulting in cell interior values above 1.25, indicated cells with a shorter lifetime in the photosynthetic membrane area. Depending on the strain, 68–149 cells were analysed (see details in Results and Discussion). For image analyses all cells in the field were analysed.

Transmission electron microscopy was performed as described elsewhere (Nevo *et al.*, 2007).

ACKNOWLEDGEMENTS

Rakefet Schwarz is supported by the Israel Science Foundation (ISF 1245/10), Yaron Shav-Tal by the European Research Council (ERC) and Yuval Garini is supported by grants from the Israel Science Foundation (ISF 51/12 and I-CORE 1902/12). We thank Rachel Levy-Drummer for statistical analysis.

SUPPORTING INFORMATION

Additional Supporting Information may be found in the online version of this article.

Figure S1. Emission spectra recorded under the microscope indicating the presence of GFP in the NblA::GFP and Free GFP strains.

Figure S2. Spectral overlap between putative donor and acceptor pairs.

Figure S3. Histograms of the time delays of *E. coli* cells expressing free GFP or NblA::GFP from the pASK-IBA3 plasmid and the control strain and mean fluorescence lifetime calculated for the different strains.

Figure S4. Sequential recruitment of confocal fluorescence cell images results in dispersed phycobilisome fluorescence.

Table S1. Strains and cloning procedures.

REFERENCES

- Adam, Z., Rudella, A. and van Wijk, K.J. (2006) Recent advances in the study of Clp, FtsH and other proteases located in chloroplasts. *Curr. Opin. Plant Biol.* **9**, 234–240.
- Ades, S.E. (2008) Regulation by destruction: design of the sigmaE envelope stress response. *Curr. Opin. Microbiol.* **11**, 535–540.
- Adir, N. (2005) Elucidation of the molecular structures of components of the phycobilisome: reconstructing a giant. *Photosynth. Res.* **85**, 15–32.
- de Alda, J.A., Lichtle, C., Thomas, J.C. and Houmard, J. (2004) Immunolocalization of NblA, a protein involved in phycobilisome turnover, during heterocyst differentiation in cyanobacteria. *Microbiology*, **150**, 1377–1384.
- Allen, M.M. and Smith, A.J. (1969) Nitrogen chlorosis in blue-green algae. *Arch. Mikrobiol.* **69**, 114–120.
- Baier, K., Nicklisch, S., Grundner, C., Reinecke, J. and Lockau, W. (2001) Expression of two *nblA*-homologous genes is required for phycobilisome degradation in nitrogen-starved *Synechocystis* sp. PCC6803. *FEMS Microbiol. Lett.* **195**, 35–39.
- Baier, K., Lehmann, H., Stephan, D.P. and Lockau, W. (2004) NblA is essential for phycobilisome degradation in *Anabaena* sp. strain PCC 7120 but not for development of functional heterocysts. *Microbiology*, **150**, 2739–2749.
- Baier, A., Winkler, W., Korte, T., Lockau, W. and Karradt, A. (2014). Degradation of phycobilisomes in *Synechocystis* sp. PCC6803: Evidence for essential formation of an NblA1/NblA2 heterodimer and its codegradation by a Clp protease complex. *J. Biol. Chem.* **289**, 11755–11766.
- Bailey, S. and Grossman, A. (2008) Photoprotection in cyanobacteria: regulation of light harvesting. *Photochem. Photobiol.* **84**, 1410–1420.
- Bakker, G.J., Andresen, V., Hoffman, R.M. and Friedl, P. (2012) Fluorescence lifetime microscopy of tumor cell invasion, drug delivery, and cytotoxicity. *Methods Enzymol.* **504**, 109–125.
- Balint, I., Bhattacharya, J., Perelman, A., Schatz, D., Moskovitz, Y., Keren, N. and Schwarz, R. (2006) Inactivation of the extrinsic subunit of photosystem II, PsbU, in *Synechococcus* PCC 7942 results in elevated resistance to oxidative stress. *FEBS Lett.* **580**, 2117–2122.
- Battesti, A. and Gottesman, S. (2013) Roles of adaptor proteins in regulation of bacterial proteolysis. *Curr. Opin. Microbiol.* **16**, 140–147.
- Bienert, R., Baier, K., Volkmer, R., Lockau, W. and Heinemann, U. (2006) Crystal structure of NblA from *Anabaena* sp. PCC 7120, a small protein playing a key role in phycobilisome degradation. *J. Biol. Chem.* **281**, 5216–5223.
- Clarke, A.K. (2012) The chloroplast ATP-dependent Clp protease in vascular plants - new dimensions and future challenges. *Physiol. Plant.* **145**, 235–244.
- Clayton, A.H., Hanley, Q.S. and Vermeer, P.J. (2004) Graphical representation and multicomponent analysis of single-frequency fluorescence lifetime imaging microscopy data. *J. Microsc.* **213**, 1–5.
- Collier, J.L. and Grossman, A.R. (1994) A small polypeptide triggers complete degradation of light-harvesting phycobiliproteins in nutrient-deprived cyanobacteria. *EMBO J.* **13**, 1039–1047.
- Digman, M.A., Caiola, V.R., Zamai, M. and Gratton, E. (2008) The phasor approach to fluorescence lifetime imaging analysis. *Biophys. J.* **94**, L14–L16.
- Dines, M., Sendersky, E., David, L., Schwarz, R. and Adir, N. (2008) Structural, functional, and mutational analysis of the NblA protein provides insight into possible modes of interaction with the phycobilisome. *J. Biol. Chem.* **283**, 30330–30340.
- Dougan, D.A., Micevski, D. and Truscott, K.N. (2012) The N-end rule pathway: from recognition by N-recognins, to destruction by AAA⁺ proteases. *Biochim. Biophys. Acta-Mol. Cell Res.* **1823**, 83–91.
- Gantt, E. (1994) Supramolecular membrane organization. In *The Molecular Biology of Cyanobacteria* (Chapter 6) (Bryant, A.D., ed.). Dordrecht, the Netherlands: Springer Kluwer Academic Publishers, pp. 119–138.
- Gao, E.B., Gui, J.F. and Zhang, Q.Y. (2012) A novel cyanophage with a cyanobacterial nonbleaching protein A gene in the genome. *J. Virol.* **86**, 236–245.
- Glazer, A.N. (1985) Light harvesting by phycobilisomes. *Annu. Rev. Biophys. Biophys. Chem.* **14**, 47–77.
- Grossman, A.R., Schaefer, M.R., Chiang, G.G. and Collier, J.L. (1993) Environmental effects on the light-harvesting complex of cyanobacteria. *J. Bacteriol.* **175**, 575–582.
- Grossman, A.R., Bhaya, D., Apt, K.E. and Kehoe, D.M. (1995) Light-harvesting complexes in oxygenic photosynthesis: diversity, control, and evolution. *Ann. Rev. Genet.* **29**, 231–288.
- Grossman, A.R., Bhaya, D. and He, Q.F. (2001) Tracking the light environment by cyanobacteria and the dynamic nature of light harvesting. *J. Biol. Chem.* **276**, 11449–11452.
- Gur, E., Biran, D. and Ron, E.Z. (2011) Regulated proteolysis in Gram-negative bacteria – how and when? *Nat. Rev. Microbiol.* **9**, 839–848.
- Hengge, R. (2009) Proteolysis of sigma(S) (RpoS) and the general stress response in *Escherichia coli*. *Res. Microbiol.* **160**, 667–676.
- Karradt, A., Sobanski, J., Mattow, J., Lockau, W. and Baier, K. (2008) NblA, a key protein of phycobilisome degradation, interacts with ClpC, a HSP100 chaperone partner of a cyanobacterial Clp protease. *J. Biol. Chem.* **283**, 32394–32403.
- Kato, H., Chibazakura, T. and Yoshikawa, H. (2008) NblR is a novel one-component response regulator in the cyanobacterium *Synechococcus elongatus* PCC 7942. *Biosci. Biotechnol. Biochem.* **72**, 1072–1079.
- Kato, H., Kubo, T., Hayashi, M., Kobayashi, I., Yagasaki, T., Chibazakura, T., Watanabe, S. and Yoshikawa, H. (2011) Interactions between histidine kinase NblS and the response regulators RpaB and SrrA are involved in the bleaching process of the cyanobacterium *Synechococcus elongatus* PCC 7942. *Plant Cell Physiol.* **52**, 2115–2122.
- Kawakami, T., Sakaguchi, K., Takechi, K., Takano, H. and Takio, S. (2009) Ammonium induced expression of the red algal chloroplast gene Ycf18, a putative homolog of the cyanobacterial *nblA* gene involved in nitrogen deficiency-induced phycobilisome degradation. *Biosci. Biotechnol. Biochem.* **73**, 740–743.
- Kehoe, D.M. (2010) Chromatic adaptation and the evolution of light color sensing in cyanobacteria. *Proc. Natl Acad. Sci. USA*, **107**, 9029–9030.
- Kirilovsky, D. and Kerfeld, C.A. (2012) The orange carotenoid protein in photoprotection of photosystem II in cyanobacteria. *Biochim. Biophys. Acta*, **1817**, 158–166.
- Kirstein, J., Moliere, N., Dougan, D.A. and Turgay, K. (2009) Adapting the machine: adaptor proteins for Hsp100/Clp and AAA⁺ proteases. *Nat. Rev. Microbiol.* **7**, 589–599.
- Lahmi, R., Sendersky, E., Perelman, A., Hagemann, M., Forchhammer, K. and Schwarz, R. (2006) Alanine dehydrogenase activity is required for adequate progression of phycobilisome degradation during nitrogen starvation in *Synechococcus elongatus* PCC 7942. *J. Bacteriol.* **188**, 5258–5265.
- Leganes, F., Forchhammer, K. and Fernandez-Pinas, F. (2009) Role of calcium in acclimation of the cyanobacterium *Synechococcus elongatus* PCC 7942 to nitrogen starvation. *Microbiology*, **155**, 25–34.
- Li, H. and Sherman, L.A. (2002) Characterization of *Synechocystis* sp. strain PCC 6803 and delta *nbl* mutants under nitrogen-deficient conditions. *Arch. Microbiol.* **178**, 256–266.
- Liberton, M., Berg, R.H., Heuser, J., Roth, R. and Pakrasi, H.B. (2006) Ultrastructure of the membrane systems in the unicellular cyanobacterium *Synechocystis* sp strain PCC 6803. *Protoplasma*, **227**, 129–138.
- Liu, H., Zhang, H., Niedzwiedzki, D.M., Prado, M., He, G., Gross, M.L. and Blankenship, R.E. (2013) Phycobilisomes supply excitations to both photosystems in a megacomplex in cyanobacteria. *Science*, **342**, 1104–1107.
- Luque, I., Zabulon, G., Contreras, A. and Houmard, J. (2001) Convergence of two global transcriptional regulators on nitrogen induction of the stress-acclimation gene *nblA* in the cyanobacterium *Synechococcus* sp. PCC 7942. *Mol. Microbiol.* **41**, 937–947.
- Luque, I., Ochoa De Alda, J.A., Richaud, C., Zabulon, G., Thomas, J.C. and Houmard, J. (2003) The NblA1 protein from the filamentous

- cyanobacterium *Tolypothrix* PCC 7601: regulation of its expression and interactions with phycobilisome components. *Mol. Microbiol.* **50**, 1043–1054.
- MacColl, R.** (1998) Cyanobacterial phycobilisomes. *J. Struct. Biol.* **124**, 311–334.
- van de Meene, A.M., Hohmann-Marriott, M.F., Vermaas, W.F. and Roberston, R.W.** (2006) The three-dimensional structure of the cyanobacterium *Synechocystis* sp. PCC 6803. *Arch. Microbiol.* **184**, 259–270.
- Mogk, A., Schmidt, R. and Bukau, B.** (2007) The N-end rule pathway for regulated proteolysis: prokaryotic and eukaryotic strategies. *Trends Cell Biol.* **17**, 165–172.
- Mullineaux, C.W.** (1999) The thylakoid membranes of cyanobacteria: structure, dynamics and function. *Aust. J. Plant Physiol.* **26**, 671–677.
- Mullineaux, C.W.** (2008) Phycobilisome-reaction centre interaction in cyanobacteria. *Photosynth. Res.* **95**, 175–182.
- Muramatsu, M. and Hihara, Y.** (2012) Acclimation to high-light conditions in cyanobacteria: from gene expression to physiological responses. *J. Plant Res.* **125**, 11–39.
- Nakamura, G., Kimura, S., Sako, Y. and Yoshida, T.** (2014) Genetic diversity of *Microcystis* cyanophages in two different freshwater environments. *Arch. Microbiol.* **196**, 401–409.
- Nevo, R., Charuvi, D., Shimoni, E., Schwarz, R., Kaplan, A., Ohad, I. and Reich, Z.** (2007) Thylakoid membrane perforations and connectivity enable intracellular traffic in cyanobacteria. *EMBO J.* **26**, 1467–1473.
- Nixon, P.J., Michoux, F., Yu, J., Boehm, M. and Komenda, J.** (2010) Recent advances in understanding the assembly and repair of photosystem II. *Ann. Bot.* **106**, 1–16.
- Nowaczyk, M.M., Sander, J., Grasse, N., Cormann, K.U., Rexroth, D., Bernat, G. and Rogner, M.** (2010) Dynamics of the cyanobacterial photosynthetic network: communication and modification of membrane protein complexes. *Eur. J. Cell Biol.* **89**, 974–982.
- Olinares, P.D., Kim, J. and van Wijk, K.J.** (2011) The Clp protease system; a central component of the chloroplast protease network. *Biochim. Biophys. Acta*, **1807**, 999–1011.
- Osanai, T., Sato, S., Tabata, S. and Tanaka, K.** (2005) Identification of PamA as a PII-binding membrane protein important in nitrogen-related and sugar-catabolic gene expression in *Synechocystis* sp. PCC 6803. *J. Biol. Chem.* **280**, 34684–34690.
- Richaud, C., Zabulon, G., Joder, A. and Thomas, J.C.** (2001) Nitrogen or sulfur starvation differentially affects phycobilisome degradation and expression of the *nblA* gene in *Synechocystis* strain PCC 6803. *J. Bacteriol.* **183**, 2989–2994.
- Ruiz, D., Salinas, P., Lopez-Redondo, M.L., Cayuela, M.L., Marina, A. and Contreras, A.** (2008) Phosphorylation-independent activation of the atypical response regulator NblR. *Microbiology*, **154**, 3002–3015.
- Salinas, P., Ruiz, D., Cantos, R., Lopez-Redondo, M.L., Marina, A. and Contreras, A.** (2007) The regulatory factor SipA provides a link between NblS and NblR signal transduction pathways in the cyanobacterium *Synechococcus* sp PCC 7942. *Mol. Microbiol.* **66**, 1607–1619.
- Sauer, R.T. and Baker, T.A.** (2011) AAA⁺ proteases: ATP-fueled machines of protein destruction. *Ann. Rev. Biochem.* **80**, 587–612.
- Sauer, J., Gori, M. and Forchhammer, K.** (1999) Nitrogen starvation in *Synechococcus* PCC 7942: involvement of glutamine synthetase and NtcA in phycobiliprotein degradation and survival. *Arch. Microbiol.* **172**, 247–255.
- Schatz, D., Nagar, E., Sendersky, E. et al.** (2012) Self-suppression of biofilm formation in the cyanobacterium *Synechococcus elongatus*. *Environ. Microbiol.* **15**, 1786–1794.
- Schmidt, R., Bukau, B. and Mogk, A.** (2009) Principles of general and regulatory proteolysis by AAA plus proteases in *Escherichia coli*. *Res. Microbiol.* **160**, 629–636.
- Schwarz, R. and Forchhammer, K.** (2005) Acclimation of unicellular cyanobacteria to macronutrient deficiency: emergence of a complex network of cellular responses. *Microbiology*, **151**, 2503–2514.
- Schwarz, R. and Grossman, A.R.** (1998) A response regulator of cyanobacteria integrates diverse environmental signals and is critical for survival under extreme conditions. *Proc. Nat. Acad. Sci. USA*, **95**, 11008–11013.
- Scruggs, A.W., Flores, C.L., Wachter, R. and Woodbury, N.W.** (2005) Development and characterization of green fluorescent protein mutants with altered lifetimes. *Biochemistry*, **44**, 13377–13384.
- Sendersky, E., Lahmi, R., Shaltiel, J., Perelman, A. and Schwarz, R.** (2005) NblC, a novel component required for pigment degradation during starvation in *Synechococcus* PCC 7942. *Mol. Microbiol.* **58**, 659–668.
- Six, C., Thomas, J.C., Garczarek, L., Ostrowski, M., Dufresne, A., Blot, N., Scanlan, D.J. and Partensky, F.** (2007) Diversity and evolution of phycobilisomes in marine *Synechococcus* spp.: a comparative genomics study. *Genome Biol.* **8**, R259.1–R259.22.
- Su, H.N., Xie, B.B., Zhang, X.Y., Zhou, B.C. and Zhang, Y.Z.** (2010) The supramolecular architecture, function, and regulation of thylakoid membranes in red algae: an overview. *Photosynth. Res.* **106**, 73–87.
- Sun, Y.S., Day, R.N. and Periasamy, A.** (2011) Investigating protein-protein interactions in living cells using fluorescence lifetime imaging microscopy. *Nat. Protoc.* **6**, 1324–1340.
- Tamary, E., Kiss, V., Nevo, R., Adam, Z., Bernat, G., Rexroth, S., Rogner, M. and Reich, Z.** (2012) Structural and functional alterations of cyanobacterial phycobilisomes induced by high-light stress. *Biochim. Biophys. Acta*. **1817**, 319–327.
- Tandeau, D.M.** (2003) Phycobiliproteins and phycobilisomes: the early observations. *Photosynth. Res.* **76**, 193–205.
- Tikkanen, M., Grieco, M., Nurmi, M., Rantala, M., Suorsa, M. and Aro, E.M.** (2012) Regulation of the photosynthetic apparatus under fluctuating growth light. *Philos. Trans. R. Soc. Lond. B Biol. Sci.* **367**, 3486–3493.
- Ting, C.S., Rocap, G., King, J. and Chisholm, S.W.** (2002) Cyanobacterial photosynthesis in the oceans: the origins and significance of divergent light-harvesting strategies. *Trends Microbiol.* **10**, 134–142.
- Tydemers, J., Mogk, A. and Bukau, B.** (2010) Cellular strategies for controlling protein aggregation. *Nat. Rev. Mol. Cell Biol.* **11**, 777–788.
- Vass, I. and Aro, E.-M.** (2007) Photoinhibition of photosynthetic electron transport. In *Primary Processes in Photosynthesis, Comprehensive Series in Photochemical and Photobiological Sciences*. (Renger, G., ed). Cambridge, UK: RSC Publishing, The Royal Society of Chemistry, pp. 393–425.
- van Waasbergen, L.G., Dolganov, N. and Grossman, A.R.** (2002) *nblS*, a gene involved in controlling photosynthesis-related gene expression during high light and nutrient stress in *Synechococcus elongatus* PCC 7942. *J. Bacteriol.* **184**, 2481–2490.
- Watanabe, M. and Ikeuchi, M.** (2013) Phycobilisome: architecture of a light-harvesting supercomplex. *Photosynth. Res.* **116**, 265–276.
- Yoshida, T., Nagasaki, K., Takashima, Y., Shirai, Y., Tomaru, Y., Takao, Y., Sakamoto, S., Hiroishi, S. and Ogata, H.** (2008) Ma-LMM01 infecting toxic *Microcystis aeruginosa* illuminates diverse cyanophage genome strategies. *J. Bacteriol.* **190**, 1762–1772.
- Yoshida-Takashima, Y., Yoshida, M., Ogata, H., Nagasaki, K., Hiroishi, S. and Yoshida, T.** (2012) Cyanophage infection in the bloom-forming cyanobacteria *Microcystis aeruginosa* in surface freshwater. *Microbes Environ.* **27**, 350–355.
- Zabulon, G., Richaud, C., Guidi-Rontani, C. and Thomas, J.C.** (2007) NblA gene expression in *Synechocystis* PCC 6803 strains lacking DspA (Hik33) and a NblR-like protein. *Curr. Microbiol.* **54**, 36–41.